Steel and Composite Structures, *Vol. 26, No. 4 (2018) 463-471*
DOI: https://doi.org/10.12989/scs.2018.26.4.463

Experimental study on a new type of assembly bolted end-plate connection

Shufeng Li*, Qingning Li, Haotian Jiang, Hao Zhang, Lei Yan and Weishan Jiang

School of Civil Engineering, Xi'an University of Architecture and Technology, Xi'an 710055, P.R. China

(*Received March 21, 2017, Revised December 10, 2017, Accepted December 12, 2017*)

Abstract. The bolted end-plate beam-column connections have been widely used in steel structure and composite structure because of its excellent seismic performance. In this paper, the end-plate bolted connection is applied in the concrete structure, A new-type of fabricated beam-column connections with end-plates is presented, and steel plate hoop is used to replace stirrups in the node core area. To study the seismic behavior of the joint, seven specimens are tested by pseudo-static test. The experimental results show that the new type of assembly node has good ductility and energy dissipation capacity. Besides, under the restraint effect of the high-strength stirrup, the width of the web crack is effectively controlled. In addition, based on the analysis of the factors affecting the shear capacity of the node core area, the formula of shear capacity of the core area of the node is proposed, and the theoretical values of the formula are consistent with the experimental value.

Keywords: bolted end-plate connection; prefabricated joint; seismic behavior; joint core zone; shear capacity

1. Introduction

With the transformation and upgrading of construction industrialization, prefabricated buildings become the development direction of the construction industry in China by virtue of the advantages of green environmental protection and high efficiency. But at present, the assembly structures used in seismic area are less, the main reason is that the previous fabricated structure failed to withstand the test of earthquakes and showed a poor overall performance, which once hindered the development of assembly structure in China. From the foreign researches (Augusto *et al*. 2016, Khoo *et al*. 2006, Hwang *et al*. 2013, Ismail *et al*. 2016, Im *et al*. 2013, Iqbal *et al*. 2016), assembly structure can indeed reach the requirements of seismic by reasonable design and some measures. In recent years, a lot of experiments are carried out by domestic scholars (Yan *et al*. 2010, Qiu and Chen 2002, Li *et al*. 2013, Cao *et al*. 2014, Zhang *et al*. 2013, Cao *et al*. 2014, Li *et al*. 2007), which also confirmed that the assembly structure has good seismic performance. The investigation of earthquake indicates that the failure of prefabricated frame structure often occurs at joint location, so it is of great significance to study the assembly nodes, which can accelerate the process of building industrialization. The bolted end-plate connection used in the steel structure and composite structure exhibits satisfactory energy dissipation capacity and ductility. But the application of end-plate connections is less in concrete structure. In this paper, based on the bolted end-plate connections used in steel structures and the study of such nodes at home and abroad, end-plate bolt connection is used in concrete structures, confined concrete with dense spiral stirrup is adopted in the beam and column. In addition, the reinforcement in the beam adopts partial prestressed reinforcement form. In the node core area, the stirrups are replaced by steel plate hoop.

*Corresponding author, Ph.D.,
E-mail: 1371757493@qq.com

2. Experimental program

Seven full scale model specimens are designed in this test, where RC-01 is the cast-in-place node and the others are the assembly node. The basic parameters of all specimens are shown in Table 1. The 4 mm -thick steel plate hoop are adopted to replace stirrups in all specimens. The pouring of the column is relatively simple. But to ensure the synergistic work of the steel hoop and the concrete, here in forcement bar should be welded inside the steel plate hoop, as shown in Fig. 1. For the construction of beam, the welding quality of the pier head and end plate is very important. The vertical welding of the pier head and end plate should be guaranteed. To ensure the welding quality, we recommend using gas shielded welding for welding. The

Fig. 1 Arrangement form of the reinforcement bar

http://www.techno-press.org/?journal=scs&subpage=6
ISSN: 1229-9367 (Print), 1598-6233 (Online)

Table 1 Details of specimens

Specimen	Strength of concrete	Cross section	Section size (mm)	Longitudinal reinforcement
column	C60	rectangle	400×400	16Φ22HRB600
RC-01	C60	rectangle	450×380	12Φ22HRB600
PAN-03	C40	I-shaped	450×380×110×150	4Φ25HTH1080 8Φ18HRB400
PAN-04	C40			
PAN-05	C40			
PAN-06	C40			
PAN-07	C40			
PAN-08	C40			

Fig. 2 The pier head connections

pier head connections are shown in Fig. 2. For the convenience of assembly, the gap between the end-plate and the column is 10 mm. The beams are adjusted to keep the beam and column at the right angle, then G-1 type high-strength grouting material is used for grouting treatment.

2.1 Test specimens

The Φ5HTH1100 high-strength spiral stirrups are used in the beam and column, the space of the stirrup is 50 mm, the interval of the encryption zone is 30 mm. The prestressed reinforcement in the beam does not pass through the node core area and the non-prestressed tendon is welded on the end-plate by the enlarged pier head, which can be seen in Fig. 2. The end-plate adopts Q390 steel, and the bolt

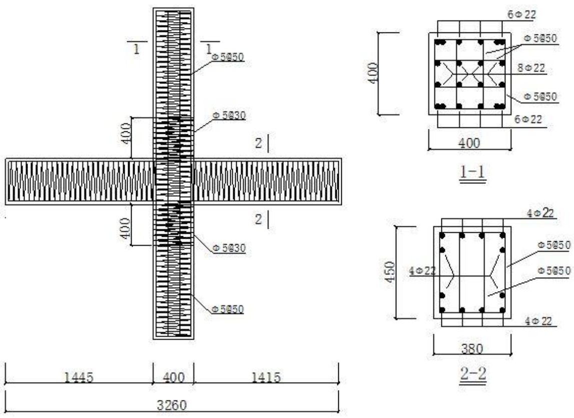

(a) Size and reinforcement of RC-01 specimen

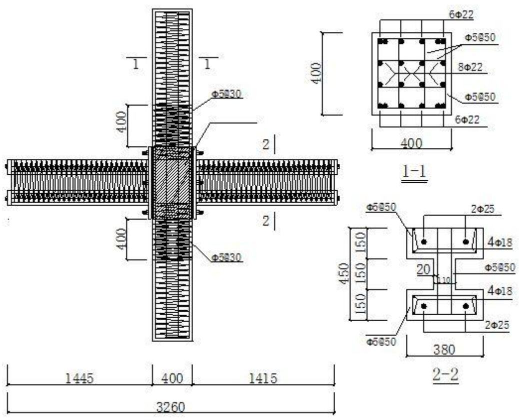

(b) Size and reinforcement of PAN-05~08 specimens

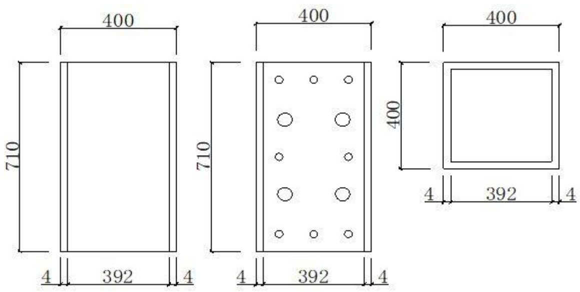

(c) Detail drawing of steel plate hoop

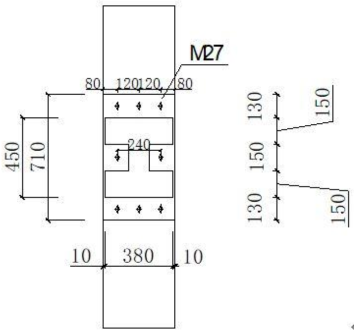

(d) Arrangement diagram of bolts

Fig. 3 Specific size and structure of specimen

Table 2 Mechanical properties of steel

Material properties	Reinforcement diameter				Thickness of steel plate
	5	18	22	25	4
Yield strength /Mpa	1157.5	451.7	698.3	1026.7	296.7
Ultimate strength /Mpa	1776.7	688.3	878.3	1161.2	448.3
Modulus of elasticity /Mpa	2.0×10^5	2.10×10^5	2.11×10^5	2.06×10^5	2.03×10^5
Percentage elongation after fracture	1.2	24	21	12	29

rod is equipped with Φ27HTH1080 prestressed bolt rod. The specific size and structure of the specimens are presented in Fig. 3. The differences among test specimens is that the PAN-07 and PAN-08 are used to set the 4 mm thick steel plate hoop instead of the stirrup in the plastic hinge area of the beam to achieve better restraint effect and realize plastic hinge transfer.

2.2 Material properties (*GB/T50081-2002*)

The material properties tests of the material used in this test are used to determine the actual mechanical properties of the material. The compressive strength of the concrete cube in the column and the cast-in-place specimen is 42 Mpa, and the compressive strength of the concrete cube used in the beam of assembly node is 28 Mpa. In addition, the tensile test is conducted for the pier head. The test results indicate that damage cannot occur at the enlarged pier head.

3. Test setup and loading history

During the test, 1200 kN axial force is applied to the top of the column by the hydraulic jack. Then the horizontal cyclic loading is applied in the horizontal direction of the top column by horizontal actuator. The mixed loading mode of force and displacement is adopted. The load is controlled by the force before the specimen yielded, and repeated only once at each control point. Then displacement-control is used after the specimen yielded, repeated three times at each control point. Load P and displacement Δ are automatically collected by TDS-602 and the P-Δ hysteresis curve is drawn. The loading device and the loading history are shown in Fig. 4.

4. Analysis on test results

4.1 Test process

Under the condition of constant axial pressure and low cyclic loading, the shear failure of the specimen RC-01 occurs in node core area due to the failure of the design. The failure modes of PAN series specimens are approximately the same, the bending failure of the beam occur in all prefabricated specimens. When the load reaches 120 kN, the bending crack appears at the beam flange which is apart from the column about 200 mm~250 mm. When the load is about 180 kN, there are slight oblique cracks in the beam web. After the non-prestressing reinforcement yielded, there are many bending cracks in the flange. At this time, the flange crack width is developed to 0.25 mm, and the diagonal crack width of the web reaches 0.1 mm. When entering the displacement control stage, with the increase of displacement and the damage accumulation of the specimen, the plastic hinge is formed at the beam end and the concrete protective layer falls off seriously. The steel plate hoop is used to wrap the beam end plastic hinge in the specimen PAN-07, PAN-08, and the region is not

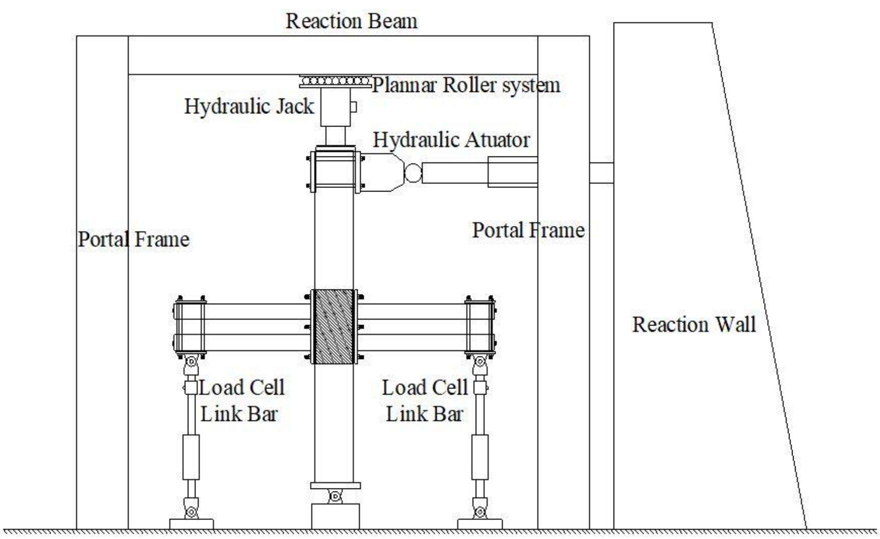

(a) Test loading device

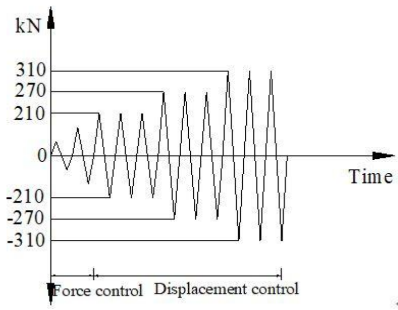

(b) Loading history

Fig. 4 Schematic diagram of test loading device and loading system

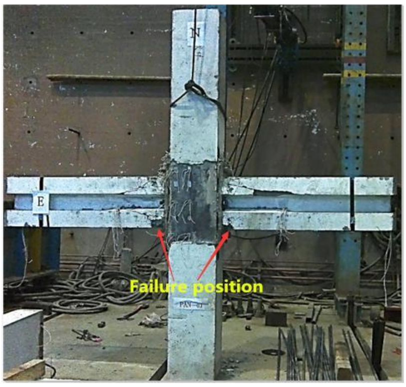

(a) PAN-03 ultimate failure mode

(b) PAN-04 ultimate failure mode

(c) PAN-05 ultimate failure mode

(d) PAN-06 ultimate failure mode

(e) PAN-07 ultimate failure mode

(f) PAN-08 ultimate failure mode

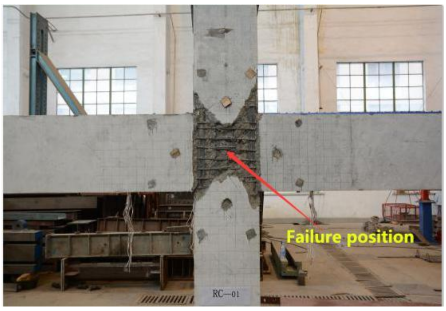

(h) RC-01 ultimate failure mode

Fig. 5 Specimens ultimate failure modes

equipped with stirrups. From the failure mode of the specimens, the plastic hinge of the beam end is transferred to the outside of the steel hoop. In the whole process, there are no obvious deformation and cracks in the column, the steel plate hoop does not show the phenomenon of slippage. Fig. 5 shows the failure modes of each specimen.

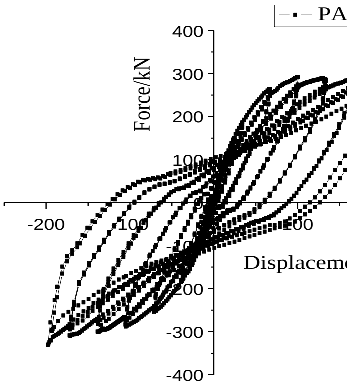

(a) PAN-03

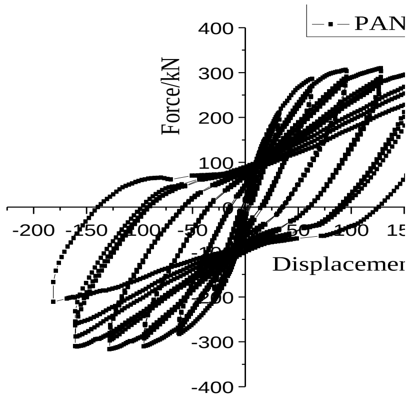

(b) PAN-04

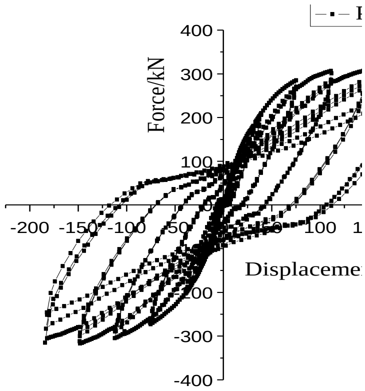

(c) PAN-05

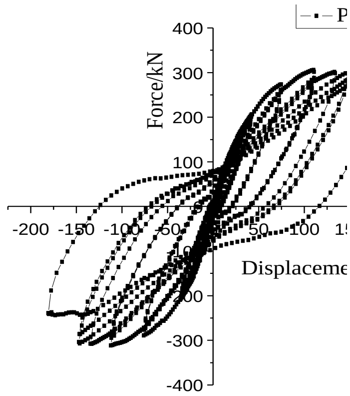

(d) PAN-06

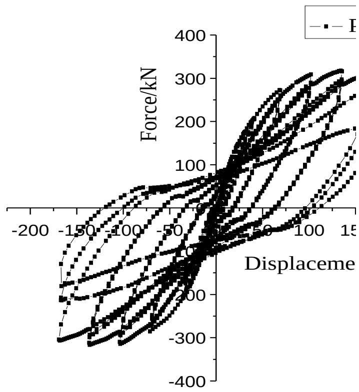

(e) PAN-07

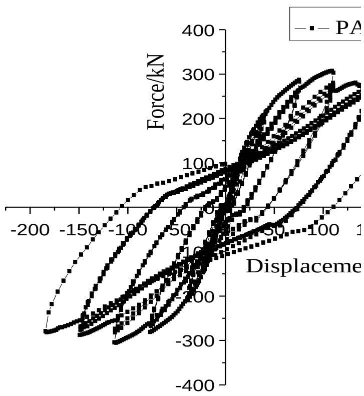

(f) PAN-08

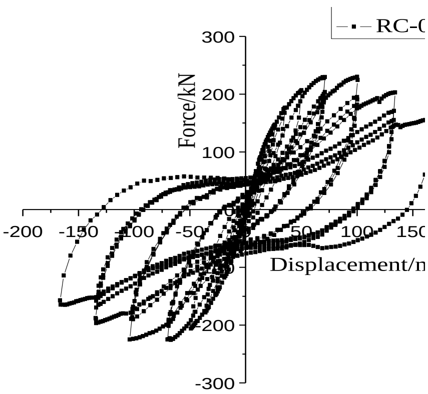

(h) RC-01

Fig. 6 Hysteresis curves of specimens

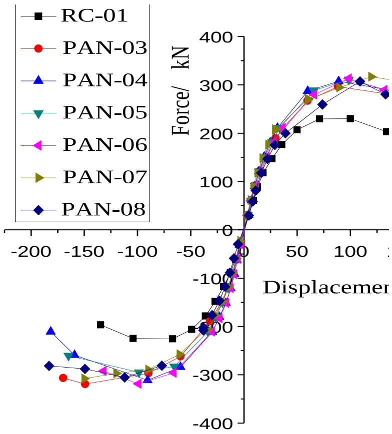

Fig. 7 Skeleton curve of specimens

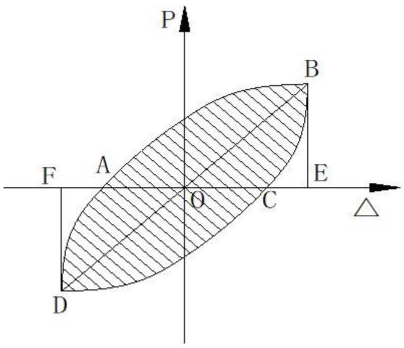

Fig. 8 Hysteresis loop energy

4.2 Hysteresis curve

The hysteresis curves of the specimens are shown in Fig. 6. Because the shear failure of the node core area occurred in the specimen RC-01, the hysteresis curve exhibits a certain shrinkage phenomenon. However, when the concrete protective layer falls off in the core area, the specimen still has a certain bearing capacity, and there is no phenomenon of bearing capacity mutation, which shows that the dense high strength spiral stirrup can provide better constraint effect for core concrete. The hysteresis curves of the assembly node are relatively plump, showing better energy dissipation capacity, and the load drops is not obvious under the same displacement, which indicates that the strength degradation of the fabricated node is small. Under the control of same displacement, because of the existence of prestress, the three hysteresis loop is close, and the stiffness is almost no degradation, the structure shows good recovery characteristics. In the late stage of loading, the strength and stiffness of the specimens degenerate rapidly, the main reason is that there is a slip between the steel plate hoop and concrete.

4.3 Skeleton curve

As can be seen from Fig. 7, the bending failure does not occur in the beam end of cast-in-place concrete specimen, and it is a typical shear failure in the core area of the node, so the specimen is not suitable for comparison. But from the skeleton curve of the assembly node, under the condition of low cyclic loading, the specimens are subjected to elastic, plastic and failure stages. The specimens experience a longer horizontal segment. After reaching the peak load when reaching the yield load, the skeleton curves decrease slowly, which indicate that the specimens have good deformation ability.

4.4 Ductility and energy dissipation capacity

In this paper, the component's energy dissipation is evaluated by equivalent viscous coefficient h_e. The calculation formulas of equivalent viscous coefficient can be seen in the Eq. (1), where S_{ABCD} is the area of hysteretic

Table 3 Ductility and energy dissipation capacity of the specimens

Specimen		Yield displacement Δ_y/mm	Limit load Δ_u/mm	Ductility factor	Energy dissipation coefficient	Equivalent viscous damping coefficient
RC-01	Front	43.19	134.07	3.1	1.687	0.268
	Back	-44.18	132.91	3.0		
PAN-03	Front	72.36	186.14	2.6	1.262	0.201
	Back	-53.4	-193.2	3.6		
PAN-04	Front	54.96	168.42	3.1	1.234	0.196
	Back	-52.44	176.99	3.4		
PAN-05	Front	52.13	163.54	3.1	1.222	0.194
	Back	-62.22	-163.54	2.6		
PAN-06	Front	50.25	177.66	3.5	1.478	0.235
	Back	-45.94	-152.31	3.3		
PAN-07	Front	59.25	160.15	2.7	1.201	0.191
	Back	-55.44	-159.3	2.9		
PAN-08	Front	55.04	152.53	2.8	1.319	0.210
	Back	-55.44	176.25	3.2		

loop, S_{OBE} and S_{ODF} are areas within OBE and ODF, as shown in Fig. 8.

$$h_e = \frac{1}{2\pi} \frac{S_{ABCD}}{S_{OBE} + S_{ODF}} \tag{1}$$

The ductility factor is defined as the ratio of limit displacement to yielding displacement, the ultimate displacement is the corresponding displacement values when the bearing capacity drops to 85% of peak value, and the yield displacement is determined according to equivalent energy method. The ductility coefficient, energy dissipation coefficient and equivalent viscosity coefficient of each specimen are shown in Table 3.

It can be seen from Table 3 that the ductility coefficients of the assembly node are between 2.6 and 3.6, the ductility coefficient of cast-in-situ reinforced concrete frame joints obtained from past test are about 2.0~5.5 (Zenunović and Folić 2012, Ma and Su 2010), the ductility coefficient of the test specimen is in the range, which indicates that the joint has good displacement ductility. The equivalent viscous damping coefficients of the assembled node are between 0.191 and 0.235 while the equivalent viscous damping coefficient of reinforced concrete joints and pure steel frame joints is 0.1 (Zeng 2008) and 0.2 (Wang *et al*. 2014), respectively. So the prefabricated node has better energy dissipation capacity. From the failure patterns, the existence of steel plate hoop result in relocation of beam plastic hinge of specimen PAN-07, PAN-08 away from the joint. But it can be seen from the bearing capacity, ductility, and energy dissipation capacity that the test piece PAN-07, PAN-08 does not exhibit good seismic performance. The steel plate hoop can only restrain the concrete of the beam end, and prevent the concrete protective layer from falling off as well as improve its rigidity.

5. Restraint effect of high-strength stirrup

Fig. 9 shows the skeleton curve of the beam end stirrup strain of assembly node specimens.

From the skeleton curve, the stirrup is only in the state of tension, and the shear is mainly undertaken by web stirrups. The flange stirrups have a certain contribution to the shear. During the initial loading, stirrup strain and shear develop linearly and the strain of stirrups is small, the reason is that the beam is in the elastic stage, and there are no cracks in the web concrete, the concrete mainly bear the shear. After the web concrete cracks, shear force previously bore by the concrete is transferred to the stirrup, and the web stirrup strain increase suddenly. But due to the restraint effect of the high-strength stirrup, the width of the web crack is effectively controlled. During the later loading, the skeleton curve tends to be flat. The strain of the stirrups and crack width of web continue to increase. The shear failure does not occur in the web, which demonstrates that the confinement effect of the high-strength stirrups greatly improves the deformation capacity of concrete.

6. Shear bearing capacity of node core area

The mechanism of the concrete in the new high-strength end plate assembly node is basically similar to that of the cast-in-place concrete structure, which is the so-called baro

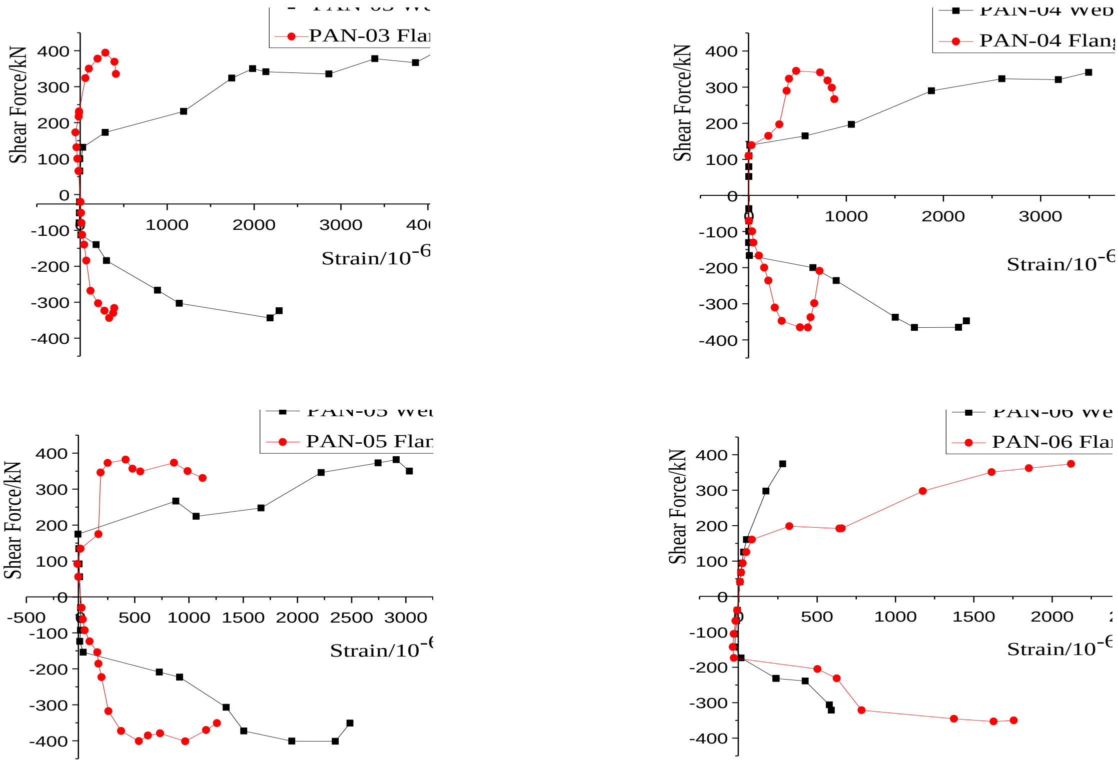

Fig. 9 Skeleton curve of beam-end stirrup

clinic pressure bar mechanism. However, due to the existence of high strength bolt pre stress and steel plate hoop, the concrete in the core area is in the three axis stress state, which greatly improves the shear capacity of concrete. Based on the study of the shear mechanism at home and abroad and the superposition principle, this paper mainly considers the contribution of bolt preload and steel plate hoop, the formula of shear capacity of the core of the assembly node is proposed.

6.1 Contribution of concrete (Nishiyama et al. 2014)

According to the experimental and theoretical analysis, in the core area of assembly node, the oblique compressive bar is formed along the diagonal direction, the shear capacity of concrete in the core area mainly depends on the compressive strength of the diagonal bar, the stress mechanism is consistent with that of ordinary concrete joint. Refer to the “code for design of concrete structures” (GB50010-2010), the equation of shear capacity of concrete in core area of assembly node is given by

$$V_c = 0.11 f_{cc} b_c h_c \tag{2}$$

Where b_c is the width of the node core area; h_c is the height of the node core area

f_{cc} is the strength of confined concrete, under the constraint of bolt preload force and axial force, the concrete in the core region is in the state of biaxial compression, according to Kupfer strength criterion, f_{cc} can be obtained from the equation as follows

$$f_{cc} = \frac{1+3.65a}{(1+a)^2} f_c \qquad (0 \le a = \sigma_1 / \sigma_2 \le 1) \tag{3}$$

According to the principle of stiffness distribution, the vertical compressive stress of concrete is obtained as

$$\sigma_1 = N \bullet \frac{E_c A_c}{E_s A_s + E_c A_c} \bullet \frac{1}{A_c} \tag{4}$$

Where N is the axial pressure column; A_s is the cross-sectional area of steel plate hoop;

A_c is the sectional area of the code zone concrete; E_c is the elastic modulus of concrete.

The lateral pressure produced by the bolt preload is expressed as

$$\sigma_2 = \frac{P}{b_c h} \tag{5}$$

Where P is the sum of the bolt preload.

6.2 Contribution of steel plate hoop

The steel plate hoop in the nodal zone has a significant effect on the shear bearing capacity of the joints, and shear force is mainly borne by the side plate hoop. (Wang *et al*. 2014) Before yielding, the steel plate hoop is in the elastic stage, and the principal tensile stress is given by

$$\sigma_1 = \frac{\sigma_{col}}{2} + \sqrt{\left(\frac{\sigma_{col}}{2}\right)^2 + \tau^2} \tag{6}$$

The principal compressive stress can be expressed as

$$\sigma_2 = \frac{\sigma_{col}}{2} - \sqrt{\left(\frac{\sigma_{col}}{2}\right)^2 + \tau^2} \tag{7}$$

According to the fourth strength theory, when the limit state is reached, the condition of shear yield can be expressed as

$$\sqrt{\sigma_1^{\,2} + \sigma_2^{\,2} - \sigma_1 \sigma_2} \le f_{yw} \tag{8}$$

f_{yw} is the tensile yield strength value of steel plate hoop.

Combining Eqs. (6), (7) and (8), the shear yield strength of the steel plate hoop can be represented by

$$\tau = \sqrt{f^2_{yw} - \sigma^2_{col}} / \sqrt{3} \tag{9}$$

It can be seen from Eq. (9) that the presence of axial pressure has a detrimental effect on the shear capacity of steel plate hoops, but related studies have shown that this effect is not obvious when using ordinary concrete and steel. So the shear strength of the steel plate hoop can be $1/\sqrt{3}$ times of the yield strength of pure shear, namely

$$\mathrm{V_w} = \frac{1}{\sqrt{3}} \sum A_{sw} f_{yw} \tag{10}$$

Where ΣA_{sw} is the area of the steel plate hoop in the direction of shear force.

The research of domestic and foreign scholar indicated that the steel plate hoop often fail to yield when the specimen failure. According to the Architectural Institute of Japanese Standards, the shear capacity of the steel plate hoop is reduced by the reduction factor of 0.5. The reduction factor of 0.5 is also adopted in this paper, so the shear bearing capacity V_w of steel plate hoop is given by

$$\mathrm{V_w} = 0.5 \times \frac{1}{\sqrt{3}} \sum A_{sw} f_{yw} \tag{11}$$

Based on the above analysis, the formula for the shear capacity of the node core area is proposed, which can be seen in Eq. (12).

$$\begin{aligned} \mathrm{V_N} &= \mathrm{V_c} + V_w \\ &= 0.11 f_{cc} b_c h_c + 0.5 \times \frac{1}{\sqrt{3}} \sum A_w f_{yw} \end{aligned} \tag{12}$$

The results of this paper and other literature adopting Eq. (12) are shown in Table 4.

As can be seen from Table 4, the theoretical value is consistent with the experimental value in other literature (Wu and Chung 2005). In this paper, the shear bearing capacity derived from Eq. (12) of the node core area is 1.3 times of the maximum shear test value, so the shear failure does occur in the node zone, which is consistent with the experimental phenomenon.

Table 4 Comparison of experimental value and theoretical calculation

Literature	Specimen	Experimental value /kN	Theoretical value /kN	Theoretical value /Experimental value
This paper	PAN-03	1522	1886	1.239
	PAN-04	1495		1.261
	PAN-05	1487		1.269
	PAN-06	1484		1.271
	PAN-07	1483		1.272
	PAN-08	1494		1.263
Other literature (Wu *et al*. 2005)	FSB-6	2679	2638	0.985
	FSB-8	2934	3045	1.037
	FSB-10	2976	2968	0.997

7. Conclusions

- From the failure mode and seismic performance of the specimens, the assembly node has good ductility and energy dissipation capacity.
- The purpose of the PAN-07 and PAN-08 specimens with steel plate hoop is to realize the plastic hinge transfer and increase the seismic behavior of the structure. From the failure mode of the specimens, the plastic hinge of the beam end is transferred to the outside of the steel hoop, however, it can be seen from the seismic indicators the specimens fail to exhibit superior seismic performance and further research remains to be done .
- In this test, the width of the web of the I-beam is small, but there is no shear failure in the web, which indicates that the deformation of the concrete can be greatly improved under the constraint of high strength stirrup.
- According to the superposition principle and the contribution of bolt preload and steel plate hoop, this paper put forward the shear capacity formula of the joint core zone and the theoretical values agree well with the experimental results, which provide reference for theoretical research and practical application.

References

Augusto, H., Castro, J.M., Rebelo, C. and da Silva, L.S. (2016), “Characterization of the cyclic behavior of the web components in end-plate beam-to-column joints”, *Procedia Eng*., **160**, 101-108.

Cao, H., Yong, B., Hua, J.M. and Li, G.R. (2014), “Tests for behavior of steel-hoop RC beam-column joints under cyclic loading”, *J. Vib. Shock*., 19, 123-128.

GB/T50081-2002 (2002), Standard for Test Method of Mechanical Properties on Ordinary Concrete.

GB/T50010-2010 (2010), Code for Design of Concrete Structures.

Hwang, H.J., Eom, T.S., Park, H.G., Lee, C.N. and Kim, H.S. (2013), “Cyclic loading test for TSC Beam – PSRC column connections”, *J. Korean Soc. Steel Constr*., **25**(6), 601-612.

Im, H.J., Park, H.G. and Eom, T.S. (2013), “Cyclic loading test for reinforced-concrete-emulated beam-column connection of precast concrete moment frame”, *ACI Struct. J*., **110**(1), 115.

Iqbal, A., Pampanin, S. and Buchanan, A.H. (2016), “Seismic performance of full-scale post-tensioned timber beam-column connections”, *J. Earthq. Eng*., **20**(3), 383-405.

Ismail, R.E.S., Fahmy, A.S., Khalifa, A.M. and Mohamed, Y.M. (2016), “Numerical study on ultimate behaviour of bolted end-plate steel connections”, *Latin Am. J. Solids Struct*., **13**(1), 1-22.

Khoo, J.H., Li, B. and Yip, W.K. (2006), “Tests on precast concrete frames with connections constructed away from column faces”, *ACI Struct. J*., **103**(1), 18-27.

Li, X., Xiao, Y., Mao W.F., Andersonet, J.C. and Zhou, T. (2007), “Experimental research on seismic behavior of reinforced concrete column-to-steel beam joints with bolted end-plate”, *J. Hunan Univ*. (*Natural Science Ed*.), **34**(2), 1-5.

Li, X.M., Gao, R.D. and Xu, Q.F. (2013), “Experimental study on high ductile joints for precast RC frame”, *J. Central South Univ*. (*Natural Science Ed*)., **8**, 3453-3463.

Ma, G.W. (2014), “Study on the combination of nodes connected composite beams and CCSHRC column bolted end Plate”, Xi’an University of Architecture and Technology, Xi’an, China.

Ma, G.Y. and Su, Y.P. (2010), “Calculation formulas for ultimate compressive strength and strain of FRP confined concrete cylinder”, *J. Hebei Univ. Sci. Technol*., **1**, 74-77.

Nishiyama, I., Fujimoto, T., Fukumoto, T. and Yoshioka, K. (2004), “Inelastic force-deformation response of joint shear panels in beam-column moment connections to concrete-filled tubes”, *J. Struct. Eng*., **130**(2), 244-252.

Qiu, Y. and Chen, Q.J. (2002), “Experimental research on the new assembly concrete filled steel tubular beam-column joint under cyclie loading”, *Guangzhou Architect*., **6**, 3-7.

Wang, L., Yan, S.J., Zheng, Y. and Zhang, C.L. (2014), “Tests on seismic behavior of joints in steel frame with steel-concrete composite beams”, *J. Harbin Inst. Technol*., **46**(4), 1-6.

Wang, Q.W., Shi, Q.X. and Tian, H.H. (2016), “Experimental study on shear capacity of SRC joints with different arrangement and sizes of cross-shaped steel in column”, *Steel Compos. Struct., Int. J*., **21**(2), 267-287.

Wu, L.Y. and Chung, L.L. (2005), “Seismic behavior of bolted beam-to-column connections for concrete filled steel tube”, *J. Constr. Steel Res*., **61**(10), 1387-1410.

Yan, W.M., Wang, W.M., Chen, S.C., Li, H.Q. and Gao, J. (2010), “Experimental study of the seismic behavior of precast concrete layered slab and beam to column exterior joints”, *Civil Eng. J*., **43**(12), 56-61.

Zeng, L. (2008), “Research on seismic behaviors and design method of steel reinforced high strength and high performance concrete frame joints”, Xi’an University of Architecture and Technology, Xi’an, China.

Zenunović, D. and Folić, R. (2012), “Models for behavior analysis of monolithic wall and precast or monolithic floor slab connections”, *Eng. Struct*., **40**, 466-478.

Zhang, D.C., Guo, Y. and Li, B.H. (2013), “Experimental studies on seismic of T-shape fabricated concrete joints with precast external steel and cast-in-place core concrete”, *Eng. Mech*., **1**, 156-162.

BU